

# Spatial and Spatio-Temporal Self-Focusing of Spin Waves in Garnet Films Observed by Space- and Time-Resolved Brillouin Light Scattering

O. Büttner, M. Bauer, S.O. Demokritov, and B. Hillebrands

*Fachbereich Physik and Zentrum für Lasermeßtechnik und Diagnostik, Universität Kaiserslautern, 67663 Kaiserslautern, Germany*

Yu.S. Kivshar

*Optical Sciences Centre, Australian National University, Canberra ACT 0200, Australia*

V. Grimalsky, and Yu. Rapoport

*T. Shevchenko Kiev State University, 252601, Kiev, Ukraine*

M.P. Kostylev, and B.A. Kalinikos

*St. Petersburg Electrotechnical University, St. Petersburg, 197376, Russia*

A.N. Slavin

*Department of Physics, Oakland University, Rochester, Michigan 48309, USA*

A new advanced space- and time-resolved Brillouin light scattering technique is used to study diffraction of two-dimensional beams and pulses of dipolar spin waves excited by strip-line antennas in tangentially magnetized garnet films. The technique is an effective tool for investigations of two-dimensional spin wave propagation with high spatial and temporal resolution. Nonlinear effects such as stationary and non-stationary self-focusing are investigated in detail. It is shown, that nonlinear diffraction of a stationary backward volume magnetostatic wave (BVMSW) beam, having a finite transverse aperture, leads to self-focusing of the beam at one spatial point. Diffraction of a finite-duration (non-stationary) BVMSW pulse leads to space-time self-focusing and formation of a strongly localized two-dimensional wave packet (spin wave bullet).

Magnetostatic spin waves in yttrium-iron garnet (YIG) films provide a superb testing ground to study linear and nonlinear wave processes in dispersive, diffractive, and anisotropic media with relatively low dissipation [1, 2]. The threshold of nonlinearity determined by the dissipation parameter is so low that a wide variety of nonlinear wave effects, like formation of envelope solitons [3], modulational [4], decay and kinetic [5] instabilities, can be observed for input microwave powers below 1 W. In films the wave process is easily accessible from the surface. Inductive probes [6, 7], thermo-optical methods [8], and Faraday rotation measurements [9] were used to study magnetostatic wave processes in YIG films. It is, however, the recently developed method of space- and time-resolved Brillouin light scattering (BLS) [10, 11, 12], which provides a major leap in this field due to its high temporal and spatial resolution, sensitivity, dynamic range and stability. Using this method it is now possible not only to reproduce all the results obtained previously for stationary wave processes, but also to investigate non-stationary nonlinear wave processes like propagation of intensive wave packets of finite duration and finite transverse aperture (pulse-beams) that are simultaneously affected by dispersion, diffraction, nonlinearity and dissipation [13].

In this paper we present the results of our investigations of nonlinear diffraction of dipolar spin waves propagating in tangentially magnetized YIG films. We show that our method allows to observe and investigate in detail new nonlinear effects such as the *stationary* one-dimensional self-focusing effect of microwave excited backward volume magnetostatic wave (BVMSW) beams leading to the formation of spatial spin wave solitons, and the *non-stationary*

spatio-temporal self-focusing effect of two-dimensional propagating wave packets leading to the formation of highly localized quasi-stable wave pulses – *spin wave bullets*. The last effect was predicted in optics [14], but the first experimental observation of this effect has been reported for the system of magnetostatic spin waves propagating in a YIG film [13].

The most interesting case to study two-dimensional nonlinear spin wave processes is the case BVMSW modes, propagating along the direction of the bias magnetic field that is oriented tangentially to the film. Here the nonlinear coefficient  $N$  is negative, while the coefficients  $D$  and  $S$  describing dispersion and diffraction are both positive (see Chapter 9 in [1]). Thus the Lighthill criterion [15] for modulational instability is fulfilled in both in-plane directions ( $SN < 0$ ,  $DN < 0$ ) and the BVMSW are susceptible to both self-modulation in the direction of propagation ( $z$ ) and to self-focusing in the transverse direction ( $y$ ).

To investigate both the spatial and the temporal properties of spin wave packets, we have developed a new experimental technique based on a standard Brillouin light scattering (BLS) setup. Spin waves are generated by a microwave input antenna. If microwaves with a frequency  $\omega_0$  are applied to the input antenna, a spin wave is launched with a wavevector determined by the dispersion relation  $\omega_0(k)$  of the spin wave. The spatial distribution is now measured by scanning the laser beam across the sample, which is performed by a motorized sample mount. In our experiment the spin waves were effectively excited in a wavevector interval

$k/ < 1200 \text{ cm}^{-1}$  (with the upper bound imposed by the width of the antenna). Thus, we investigate the light scattered in forward direction to achieve a high sensitivity in this low-wavevector regime.

Temporal resolution is added by using a time correlated single photon counting method similar to time-of-flight measurements in, e.g., mass spectroscopy. As the frequency selecting device we use a tandem Fabry-Perot interferometer in multipass configuration (for a detailed description see [10]). A pulse generator generates pulses of typically 10–30 ns duration with a repetition rate of 1 MHz. Each pulse is sent to a microwave switching device to create a pulsed microwave field and to generate a spin wave pulse. If the spin wave pulse crosses the laser spot, light is inelastically scattered, and an inelastically scattered photon is detected. A special counter and a memory array are used to measure the elapsed time between the launch of the spin wave pulse and the arrival at the position of the laser spot and thus to measure the temporal variation of the spin wave intensity at the current position of the laser spot. By repeating the procedure for different positions of the laser spot on the sample with a mesh size of typically 0.1 mm, a two-dimensional map of the spin wave intensity is constructed for each value of delay time. We arrange the data in a digital video animation with each frame representing the spatial distribution of the spin wave intensity for a given delay time [16]. A lower limit of about 2 ns on the time resolution is imposed by the intrinsic time resolution of the BLS spectrometer.

The samples were mounted on a standard microstrip-transducer structure with an input antenna of width  $50 \mu\text{m}$  and length 2.5 mm. The antenna is connected to a high speed switcher for the pulsed measurements which allows microwave pulses of a time duration  $T \geq 10 \text{ ns}$ . The switcher in turn is connected to a generator / network analyzer / amplifier unit, which provides a microwave input power of up to 1 W.

Evidence of nonlinear self-focusing of dipolar spin wave beams was presented in our previous short paper [17], where spectrally narrow BVMSW beams in a narrow waveguide (width 2 mm) were studied. One of the results was the appearance of a snake-like structure in the data which is caused by the interaction of transverse waveguide modes [18]. This structure is caused by the influence of the lateral boundaries of the waveguide. Different width-modes of the waveguide, excited by the microwave antenna, propagate with different phase velocities, and interfere with each other creating a snake-like pattern in the spin wave intensity in the

waveguide.

To exclude the effect of boundaries in the measurements of self-focusing presented here, a wide  $\text{Lu}_{0.96}\text{Bi}_{2.04}\text{Fe}_5\text{O}_{12}$  (BIG) sample (width 10 mm) was used. The sample was cut out of the same BIG disc from which the sample in [17] was made. In this experiment the static magnetic field was  $H = 2090 \text{ Oe}$ , the carrier frequency was  $f_0 = 8450 \text{ MHz}$ , and the resulting carrier wavevector was  $k_{0z} = 300 \text{ cm}^{-1}$ . The input power was  $P_{in} = 10 \text{ mW}$  in the linear and up to  $P_{in} = 600 \text{ mW}$  in the nonlinear case. In Fig. 1a,b the experimentally measured spin wave intensity distribution is shown for different values of the input power. The intensity maps are corrected for attenuation as is described in [17], and the data is normalized to the maximum power in each map. The antenna is oriented along the y-direction and located on the left at  $z = 0$ . In the linear case, displayed in Fig. 1a, the spin wave amplitude slightly changes due to the effect of the diffraction which causes a beam divergence during propagation, so that the spin wave intensity is distributed over a wider range with increasing distance from the antenna. In the nonlinear case the propagation of the spin waves is very different (Fig. 1b). The beam no longer diverges. It converges to a small diameter while the spin wave amplitude increases and a clear focus of spin wave intensity is observed at the point  $z = 2 \text{ mm}$ ,  $y = 2 \text{ mm}$ . This is the result of the competition between diffraction and nonlinearity, and it can be approximately interpreted as a spatial soliton of a higher order [19]. Since the spin wave beam loses energy due to dissipation during propagation, the beam finally diverges when its amplitude becomes so small, that the diffraction effect dominates, as is the case for  $z > 2.6 \text{ mm}$  in Fig. 1b.

In the experiments discussed above only stationary effects of the spin wave propagation were studied. In this case dispersion played no role. If, however, the propagation of short pulses is considered, the dispersion causing the spreading of a wave packet in the propagation direction in the linear case might influence the mode propagation significantly. To measure the real two-dimensional spatio-temporal self focusing, we used a large YIG sample (thickness  $7 \mu\text{m}$ , width 18 mm, length 26 mm) with a FMR linewidth of  $2\Delta H = 0.6 \text{ Oe}$ . The static magnetic field was  $H = 2098 \text{ Oe}$ , and the carrier frequency was chosen to be  $f_0 = 7970 \text{ MHz}$  which results in a carrier wavevector  $k_{0z} = 70 \text{ cm}^{-1}$ . The duration of the microwave input pulse was chosen to be  $T = 29 \text{ ns}$ .

Figures 2a,b show the distribution of the spin wave intensities for the above parameters and for two different input powers:  $P_{in} = 10 \text{ mW}$  in the linear (Fig. 2a) and  $P_{in} = 700 \text{ mW}$  in the nonlinear regime (Fig. 2b). The upper part of each panel shows the spin wave intensity in a three-dimensional plot for five different propagation times as indicated in the figure. The data are normalized to the maximum power in each graph. The lower parts shows the cross-sections of the wave packets at half-maximum power. In the linear case, the diffraction and the dispersion cause the broadening of the initial wave packet perpendicular to and along the propagation direction, while the amplitude decreases due to dissipation. Here diffraction is considerably larger than dispersion, so that the broadening of the wave packet in the transverse direction is much more pronounced than in the direction of propagation.

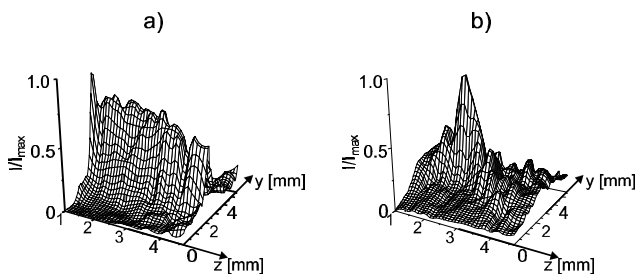


Fig. 1: Stationary self-focusing of BVMSW beams in a large BIG sample: experimental distributions of the spin wave normalized intensity in the film plane for the linear (a) and nonlinear (b) regime are shown. A clear self-focusing maximum is seen at the point ( $z = 2.5 \text{ mm}$ ,  $y = 3 \text{ mm}$ ) in the nonlinear regime.

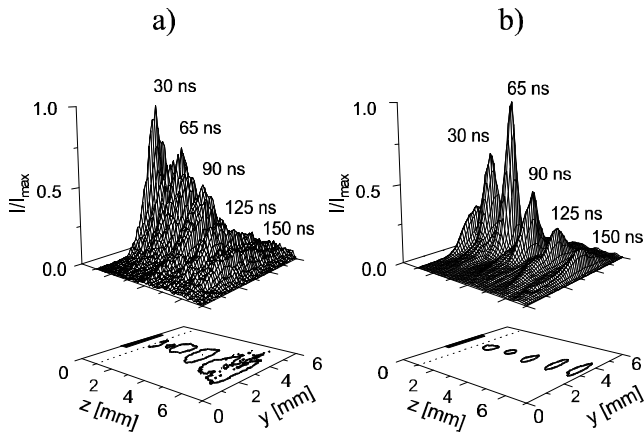


Fig. 2: Non-stationary self-focusing of a two-dimensional BVMSW packet in a large YIG film. The upper parts of the pictures show the spin wave intensity distribution in the film created by the propagating pulse of the duration  $T = 29$  ns at five successive moments after the moment of a pulse launch from the antenna as indicated in the figure. The lower parts of the panels each show the cross-sections of the propagating pulse at half-maximum power. Panels (a) and (b) show experimental data for linear and nonlinear regimes. Spatio-temporal self focusing is clearly seen for  $T = 65$  ns in the nonlinear regime.

The behavior of the wave packets in the nonlinear case is quite different (Fig. 2b). Here the initial high-amplitude wave packet starts to converge, and its amplitude is increasing. Theory (see e.g., [20]) predicts that in the two-dimensional case a stable equilibrium between dispersion, diffraction, and nonlinearity is not possible, and nonlinear self-focusing of the wave packet with high enough initial energy should lead to a wave collapse, i.e., all the energy of the packet will be concentrated at one spatial point. In a real medium with dissipation collapse is, of course, avoided, as the wave packet loses energy. Therefore, in a certain interval of propagation distances, nonlinear collapse is stabilized by dissipation, and a quasi-stable strongly localized two-dimensional wave packet, a *spin wave bullet*, is formed. The existence of stable two- and three-dimensional wave packets in a focusing media, where collapse is stabilized by saturation of nonlinearity, has been predicted for optical wave packets in [14].

In conclusion, a newly developed space- and time-resolved BLS technique was applied for the study of stationary and

non-stationary *nonlinear* self focusing of BVMSW beams. For the first time formation of highly localized quasi-stable two-dimensional packets of spin waves, *spin wave bullets*, has been observed and investigated.

Support by the Deutsche Forschungsgemeinschaft and the National Science Foundation (Grant DMR-9701640) is gratefully acknowledged.

#### References

- [1] P.E. Wigen (ed.) *Nonlinear Phenomena and Chaos in Magnetic Materials* (World Scientific, Singapore, 1994).
- [2] M.G. Cottam (ed.), *Linear and Nonlinear Spin Waves in Magnetic Films and Superlattices*, (World Scientific, Singapore 1994).
- [3] B.A. Kalinikos, N.G. Kovshikov, A.N. Slavin, *Sov. Phys. JETP Lett.* 38, 138 (1983).
- [4] B.A. Kalinikos, N.G. Kovshikov, A.N. Slavin, *Sov. Tech. Phys. Lett.* 10, 392 (1984).
- [5] P.E. Zilberman, S.A. Nikitov, A.G. Temiryazev, *Sov. Phys. JETP Lett.* 42, 110 (1985).
- [6] N.P. Vlannes, *J. Appl. Phys.* 61, 416 (1987).
- [7] A.B. Valyavsky, A.V. Vashkovsky, A.V. Stal'makov, V.A. Tyulyukin, *Sov. Phys. Tech. Phys.* 34, 616 (1989).
- [8] O.V. Geisau, U. Netzelmann, S.M. Rezende, J. Pelzl, *IEEE Trans. Mag.* 26, 1471 (1990).
- [9] A.A. Solomko, Y.A. Gaidai, O.V. Kolokoltsev, *Abstracts of ICM-94*, p 368, Warsaw, Poland (1994).
- [10] B. Hillebrands, *Rev. Sci. Instr.* 70, 1589 (1999).
- [11] O. Büttner, M. Bauer, A. Rueff, S.O. Demokritov, B. Hillebrands, A.N. Slavin, M.P. Kostylev, B.A. Kalinikos, submitted to *Ultrasonics*.
- [12] M. Bauer, O. Büttner, S.O. Demokritov, B. Hillebrands, to be submitted to *Rev. Sci. Instr.*
- [13] M. Bauer, O. Büttner, S.O. Demokritov, B. Hillebrands, V. Grimalsky, Yu. Rapoport, A.N. Slavin, *Phys. Rev. Lett.* 81, 3769 (1998).
- [14] Y. Silberberg, *Opt. Lett.* 15, 1282 (1990).
- [15] M.J. Lighthill, *J. Inst. Math. Appl.* 1, 269 (1965).
- [16] Video sequences in the AVI format can be downloaded from our home page [http://www.physik.uni-kl.de/w\\_hilleb](http://www.physik.uni-kl.de/w_hilleb).
- [17] M. Bauer, C. Mathieu, S.O. Demokritov, B. Hillebrands, P.A. Kolodin, S. Sure, H. Dötsch, V. Grimalsky, Yu. Rapoport, A.N. Slavin, *Phys. Rev. B* 56, R8483 (1997).
- [18] O. Büttner, M. Bauer, C. Mathieu, S.O. Demokritov, B. Hillebrands, P.A. Kolodin, M.P. Kostylev, S. Sure, H. Dötsch, V. Grimalsky, Yu. Rapoport, A.N. Slavin, *IEEE Trans. Magn.* 34, 1381 (1998).
- [19] G.P. Agrawal, *'Nonlinear Fiber Optics'*, Academic Press (1989), Fig. 5.6.
- [20] L. Berge, *Physics Reports* 303, 260 (1998).